

Supplementary Information

Embedding an esterase mimic inside polyester to realize rapid and complete degradation without compromising the utility

Yanfen Wu,^a Jing Tian,^{a,c} Minmin Sun,^b Lizeng Gao,^b Jun Xu,^{a,*} and Zhiqiang Niu^{a,*}

^aDepartment of Chemical Engineering, Tsinghua University, Beijing 100084, China

^bCAS Engineering Laboratory for Nanozyme, Key Laboratory of Biomacromolecules, Institute of Biophysics, Chinese Academy of Sciences, Beijing, 100101, China

^cSchool of Mechanical Engineering, Ningxia University, Yinchuan 750021, Ningxia, China

*E-mail: jun-xu@tsinghua.edu.cn; niuzq@tsinghua.edu.cn

Table of Contents:

1. Materials and Methods
2. Characterizations
3. Supplementary Figures
4. Supplementary Tables
5. References

1. Materials and Methods

Synthesis of Zn₂L: The binuclear complexes were prepared according to previously reported procedures.¹ In detail, a methanol solution of 1,3-diamino propane (1 mmol, 84 μ L) was added dropwise into a methanol solution of Zn(NO₃)₂ 6H₂O (0.3 g, 1 mmol, 5 mL) and 4-tert-Butyl-2,6-diformylphenol (0.206 g, 1 mmol, 5 mL) under stirring. The resulting solution was refluxed for 1 h under stirring and cooled down to room temperature. Yellow solid precipitated from the solution after standing overnight. The yellow precipitate was collected by filtration and vacuum drying. ¹H NMR (400 MHz, MeOD-d₄, δ): 8.55 (s, 4H, N=CH), 7.72 (s, 4H, Ar H), 4.06 (t, 8H, N-CH₂), 2.18 (m, 4H, CH₂), 1.36 (s, 18H, C-(CH₃)₃). Anal. Calcd (%) for C₃₀H₃₈N₆O₈Zn₂: C, 48.42; H, 5.38; N, 11.29. Found: C, 48.41; H, 5.24; N, 11.30. IR (DRIFTS, cm⁻¹): 1636 (s), 1560 (s), 1471 (s), 1442 (s), 1415(s), 1365 (m), 1336 (m), 1250 (m), 1311(w), 1250(m), 1233 (m), 1122 (m), 1084 (m), 1032 (m), 935 (w), 837 (w), 774 (m). HR-MS (ESI) m/z: [M]²⁺ 309.1.

Preparation of composites: PBAT (TH801T) was supplied in pellet form by Blue Ridge Tunhe Sci. & Tech. Co., Ltd., Xinjiang, China. Before compounding, PBAT pellets and Zn₂L were dried under vacuum at 50 °C for 24 h to remove moisture. 1 wt% and 5 wt% Zn₂L were premixed with dried PBAT, respectively. The mixtures were then melted and extruded using a co-rotating twin-screw extruder (HAAKE Rheomex PTW 16/25 OS MK2, ThermoElectric) with a screw diameter of 16 mm and a length/diameter ratio of 40. The twin-screw extruder has a PTW die with an exit diameter of 3 mm. The temperature of the twin-screw extruder was set at 110 °C, 120 °C, 140 °C, 160 °C, 170 °C, 170 °C, 170 °C, 165 °C, 155 °C, and 150 °C in sequence from the feed section to the die. The screw speed was 120 rpm and the feeding frequency was 2.5 Hz. The composite strands extruded from the twin-screw extruder were air-cooled and fed into a pelletizer (VariCut, ThermoElectric) to obtain pellets with a uniform size. The obtained pellets of the composites were used for blown films. A single screw extruder (HAAKE Rheomex 19/25 OS, ThermoElectric) with three heating zones and a blown

film die was used to produce the films. A blown film die with an outer diameter of 25 mm and an inner diameter of 24 mm was used. The temperature of the extruder was set at 110 °C, 125 °C, 150 °C, and 135 °C from the feed section to the die. The screw speed was 20 rpm. The blow-up ratio was 3.5, and the thicknesses of the obtained films were 20–80 μm.

PBAT hydrolysis: PBAT pellets were provided by Xinjiang Blue Ridge Tunhe Sci.&Tech. Co., Ltd. In the catalytic hydrolysis of PBAT, raw PBAT pellets were micronized and sieved to 80 μm powder for experiments. PBAT/Zn₂L films were cut into 1×1 mm² pieces for hydrolysis experiments. The hydrolysis of PBAT was carried out at 60 °C in a 20 mL vial containing NaOH aqueous solution (10 mL, pH 8), PBAT (20 mg or 40 mg), and Zn₂L catalyst (1–10 wt%). The hydrolysis process was monitored by taking out aliquots from the reaction solution for ¹H NMR analysis. The pH of the solution was maintained constant by regular testing and addition of lye.

Simulated composting: Laboratory-scale industrial composting experiments were conducted on the prepared samples following the ASTM D5338-15 standard. The composting soil I and soil II were purchased from a composting plant in Shijiazhuang (China) and from Shandong Baoprati Agricultural Technology Company Ltd., respectively, and screened using a 10-mesh sieve before use. Polymer films in 20×20 mm² were placed into a microporous filter with a pore size of 0.8 mm and then placed in composting soils inside an oven at 58°C. The PBAT samples were periodically taken out and any fragments larger than the pore size of the microporous mesh were collected. The PBAT membranes were then weighed to determine the degree of degradation after cleaning surface, washing and vacuum drying.

In vitro cytotoxicity assay: Cell viability assay was performed using a Cell Counting Kit-8 assay (CCK-8, Dojindo Molecular Technologies) to analyze the in vitro cytotoxicity of PBAT and PBAT/Zn₂L. PBAT, PBAT/Zn₂L (1 wt%), and PBAT/Zn₂L (5 wt%) were aseptically treated with 75% alcohol and then spread onto a 96-well plate.

A549 cells (at a density of 2×10^4 cells per well), L929 cells (at a density of 1.5×10^4 cells per well), or RAW267.4 cells (at a density of 3×10^4 cells per well) were plated onto the surface of PBAT or PBAT/Zn₂L in separate 96-well plates and allowed to settle overnight for adherence. After a 24 h incubation, the morphological characteristics of these three cell types were observed under a microscope. Cell viability was determined using CCK-8 according to the manufacturer's instructions, and the absorbance at 450 nm was measured using a microplate reader.

Assessment of solution pH variations: To compare the hydroxide uptake capacity of PBAT and PBAT/Zn₂L, we investigated the pH variations in solution under static conditions. The films of PBAT, PBAT/Zn₂L (1 wt%), and PBAT/Zn₂L (5 wt%) were cut into pieces (2×2 cm² with a thickness of 0.20 ± 0.02 mm) and separately immersed into 20 mL of NaOH aqueous solution (pH 8.1) in vials. The vials were sealed and placed in a dark environment at room temperature. After a predetermined period of time, the pH of the aqueous solution was evaluated using pH-indicator strips (MQuant[®], 6.5–10.0).

2. Characterizations

The Fourier transform infrared (FTIR) spectroscopy was performed using a Bruker Vertex 70 FT-IR spectrometer. Thermogravimetric analysis (TGA) was conducted using a DTG-60H apparatus of Shimadzu to evaluate thermal stability of PBAT in the temperature range of 25–700 °C at a heating rate of 10 °C min⁻¹ under N₂. Small-angle X-ray scattering (SAXS) was recorded using a NANOSTAR U SAXS instrument (Bruker) with a wavelength of $\lambda = 0.154$ nm, and q ranging from 0.07 to 2.3 nm⁻¹, where $q = 4\pi\sin\theta/\lambda$ represents the effective scattering vector. This technique was employed to probe the microscopic crystal structure of PBAT. The surface morphology and elemental content of PBAT samples were analyzed using a cold field emission scanning electron microscope (Hitachi SU8010) at an accelerating voltage of 10 kV (15 kV for EDS). Prior to analysis, the samples were coated with a layer of gold using a sputter coater. To determine the molecular weight and dispersity of PBAT, a 1 mg mL⁻¹ solution of PBAT in THF was prepared and analyzed using an Agilent PL-GPC 220 gel permeation chromatograph with a refractive index (RI) detector. The molecular weight response was calibrated with monomodal, linear polystyrene standards. Tensile tests of the samples were conducted using a universal testing machine (UTM-1432 from Chengde Jinjian Testing Instrument Co., Ltd.) following the standard GB 13022-91 (Type II) at a crosshead speed of 50 mm min⁻¹. At least five specimens were tested for each group of tests. The spherulite growth of samples was observed using an Olympus BX-41 polarized optical microscopy (POM) under crossed polarizers with a 530 nm γ compensator. Isothermal crystallization was carried out on a Linkam LTS420 hot stage. All of the samples were heated to 180 °C for 3 min to erase the thermal history and then quenched to 115 °C for isothermal crystallization. Water contact angles of PBAT and Zn₂L were measured using an OCAH20 instrument (Dataphysics Ltd., Germany) to determine the surface hydrophobicity. The measurements were repeated at least three times for each specimen. Elemental analyses (C, H, N) were carried out on a vario EL III analyzer to determine the purity of synthesized catalysts. Inductively coupled plasma optical emission spectroscopy (ICP-OES) measurements were conducted using a

Thermo X Series 2 instrument. X-ray photoelectron spectroscopy (XPS) measurements were carried out on an AXIS Supra+(Shimadzu) using Al K α X-rays as the excitation source at a voltage of 15 kV. All binding energies were referenced to the C 1s peak (284.8 eV). In order to determine the ratio of the aliphatic segment and the aromatic segment of the PBAT raw material, ^1H NMR was used to detect the hydrolysis products after completely hydrolyzed at 60 °C in an alkaline solution (pH 14). The determination of water absorption was performed according to the ISO 62:2008 standard. The fully dried samples were immersed in distilled water at room temperature and weighed after 24 hours. The water absorption mass fraction of the samples was calculated by dividing the mass difference before and after immersion by the initial mass. The organic carbon content of the composting soil was determined according to the standard NY/T 1121.6-2006. The cation exchange capacity was obtained using the leaching-spectrophotometric method described in the standard HJ889-2017. The total nitrogen content was determined using an automatic Kjeldahl analyzer. The water holding capacity was obtained using the cutting ring method (LYT1215-1999). The pH was analyzed using the potentiometric method (NY/T 1121.2-2006), and particle size distribution was determined using the density meter method (NY/T 1121.3-2006). To explore the interaction between model esters and the catalyst, diffuse reflection infrared Fourier transform spectroscopy (DRIFTS) experiments were performed on Thermo Nicolet iS50 equipped with a diffuse reflection accessory (Harrick Inc.). After the model molecules (butyl hexanoate or butyl benzoate) were fully mixed with the catalyst, the sample was heated up to remove the physisorbed esters. The X-ray absorption fine structure (XAFS) spectra at Zn *K*-edge were acquired at the 4B9A station in Beijing Synchrotron Radiation Facility (BSRF), operated at 2.5 GeV with a maximum current of 250 mA. The data for Zn₂L and embedded Zn₂L were recorded in fluorescence excitation mode using a Lytle detector. Zn foil, ZnO and Zn(NO₃)₂·6H₂O were used as reference materials and the data were measured in transmission mode using an ionization chamber. The acquired extended X-ray absorption fine structure (EXAFS) data were processed according to standard procedures using the ATHENA program

integrated within the IFEFFIT (1.2.12) software packages.² The k^3 -weighted EXAFS spectra $\chi(k)$ were Fourier-transformed in a k -range of 3.0–12.5 Å⁻¹ for the Zn K -edge with a Kaiser-Bessel window function. ¹H nuclear magnetic resonance (NMR) (400 MHz) was acquired on AVANCE III (Bruker) to analyze the products of PBAT hydrolysis. The ¹H NMR samples were prepared following the method described in the previous literature.³ The monomer products of PBAT hydrolysis are sodium terephthalate, butanediol (BDO) and sodium adipate. The peak positions of the monomers are shown in the Figure S1. The molar quantity of the analyte (n_{analyte}) in the reaction solution was calculated via the equation below^{4,5}:

$$n_{\text{analyte}} = \frac{I_{\text{analyte}}}{I_{\text{standard}}} \times \frac{N_{\text{standard}}}{N_{\text{analyte}}} \times \frac{m_{\text{standard}}}{M_{\text{standard}}} \times \frac{10}{0.1}$$

The yield of the monomer was calculated by the equation below:

$$Yield = \frac{n_{\text{analyte},t}}{n_{\text{analyte},e}} \times 100\%$$

We used the amount of butanediol to calculate the conversion of PBAT. The I_{standard} and I_{analyte} represent the peak areas of standard (Maleic acid, MA) and analyte (BDO), respectively. The m_{standard} and M_{standard} represent the mass and mole weight of MA, respectively. The N_{standard} and N_{analyte} represent the number of protons corresponding to the standard and the analyte peak, respectively. The $n_{\text{analyte},t}$ and $n_{\text{analyte},e}$ represent the amount of the analyte at the reaction time of t and at the end of the reaction, respectively.

Differential scanning calorimetry (DSC) was performed on a Q5000 IR of TA Inst. to evaluate the change of PBAT crystallinity after the addition of Zn₂L. The sample was firstly heated up from room temperature to 180 °C, and the temperature was kept at 180 °C for 5 min. Then, it was subsequently cooled to 10 °C. The second stage of thermal treatment was performed by heating up the sample to 180 °C. The ramping and cooling rates of the process are both 10 °C min⁻¹. The degree of crystallinity (X_c) was calculated by the following equation⁶:

$$X_c = \frac{\Delta H_f}{(1 - \omega)\Delta H_f^0} \times 100\%$$

ΔH_f : the enthalpy of melting

ΔH_f^0 : the standard enthalpy of melting for a 100% crystalline PBAT

ω : the weight percentage of the catalysts (^tBu-Zn₂L)

ΔH_f was calculated by integrating the endothermic melting peak of DSC, and ΔH_f^0 was taken from literature as 114 J/g.⁷

3. Supplementary Figures

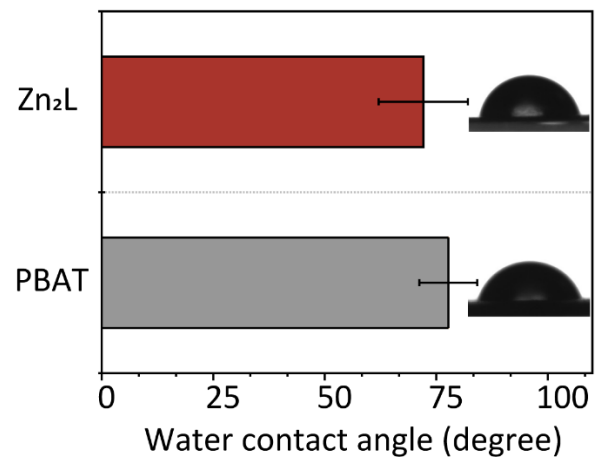


Fig. S1 Water contact angles of PBAT and Zn₂L.

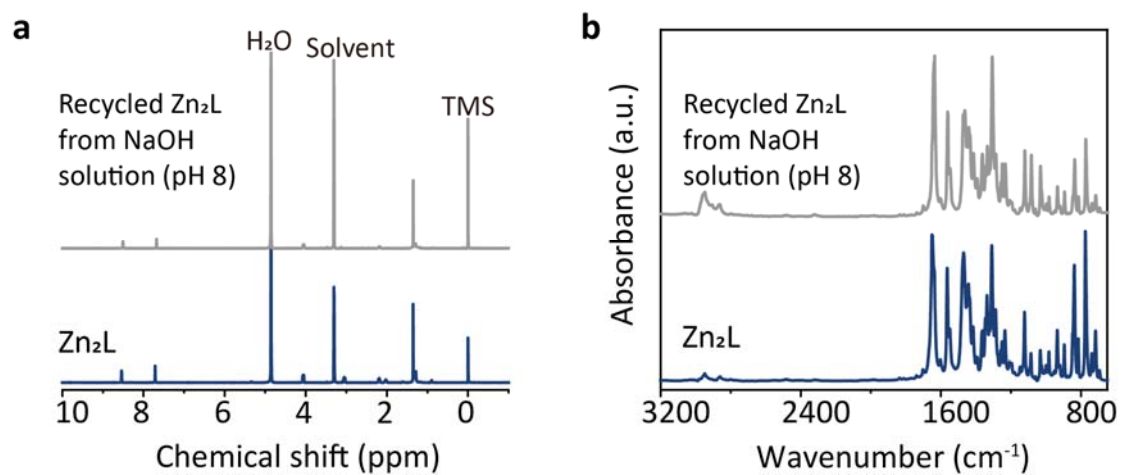


Fig. S2 ^1H NMR spectra (a) and DRIFT spectra (b) of Zn_2L and recycled Zn_2L . 20 mg of Zn_2L was dispersed in 100 mL of NaOH aqueous solution (pH 8) and stirred at 60 °C for 5 days. Then, Zn_2L was collected from the NaOH aqueous solution (pH 8) by centrifugation and vacuum-drying.

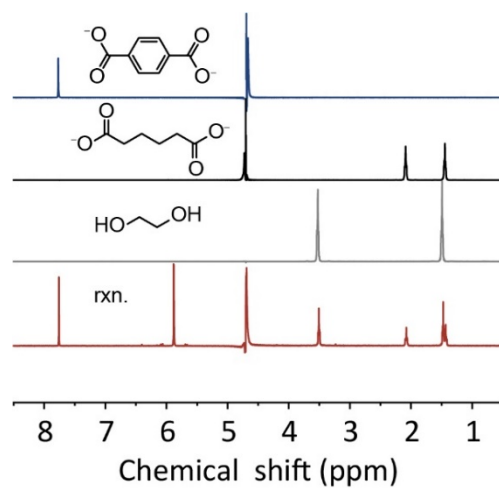


Fig. S3 ¹H nuclear magnetic resonance (NMR) spectra of the hydrolysis products. The signals at $\delta=4.7$ ppm and $\delta=5.9$ ppm are assigned to H₂O and sodium maleate, respectively.

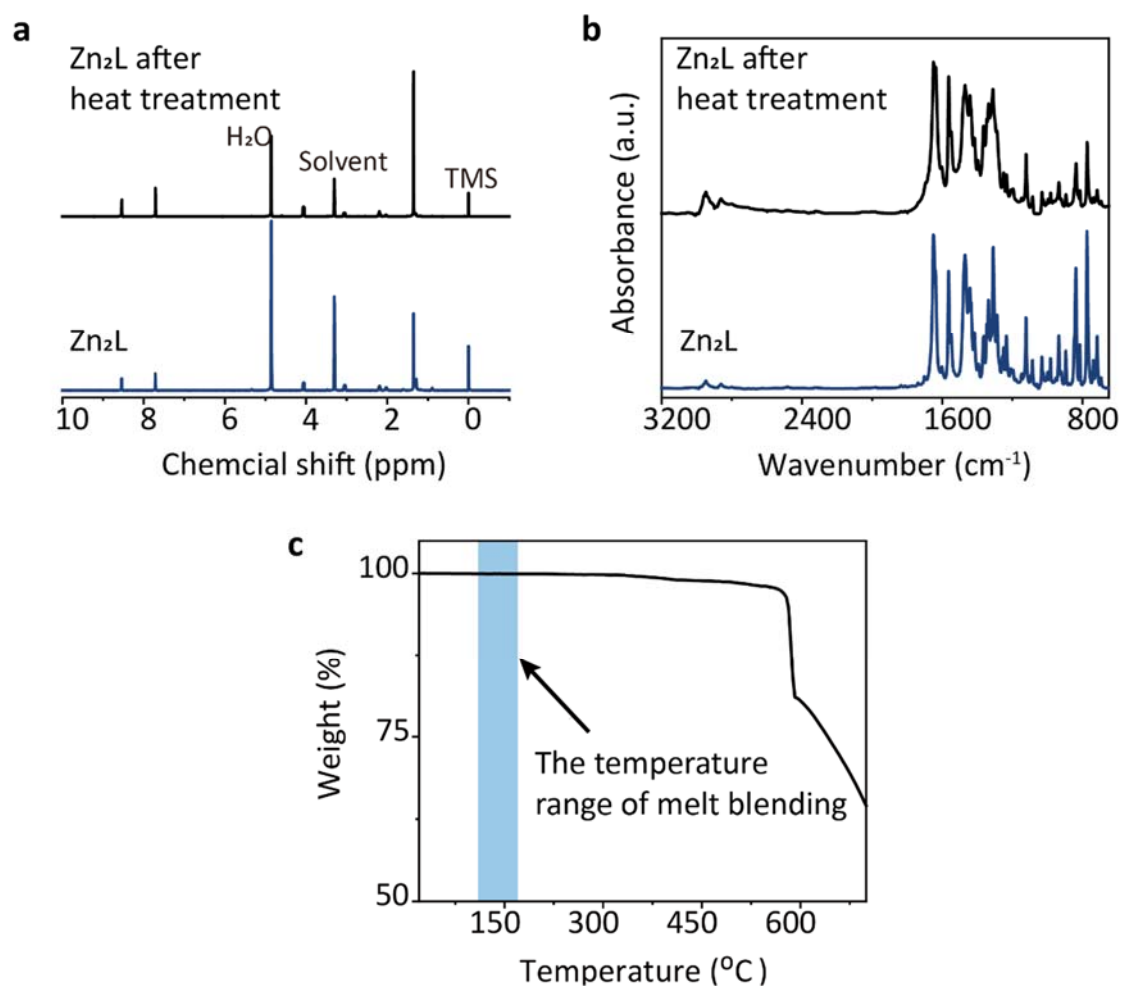


Fig. S4 ¹H NMR spectra (a) and DRIFT spectra of Zn₂L and Zn₂L (b) after heat treatment. (c) Thermogravimetric analysis curve of Zn₂L. The Zn₂L was treated in air at 170 °C for 30 minutes in a flask. The heat treatment temperature is the maximum set temperature of the twin-screw extruder. The ¹H NMR and DRIFT spectra of Zn₂L after the heat treatment are both identical to those of pristine Zn₂L. The weight of Zn₂L remains constant throughout the temperature range of melt blending.

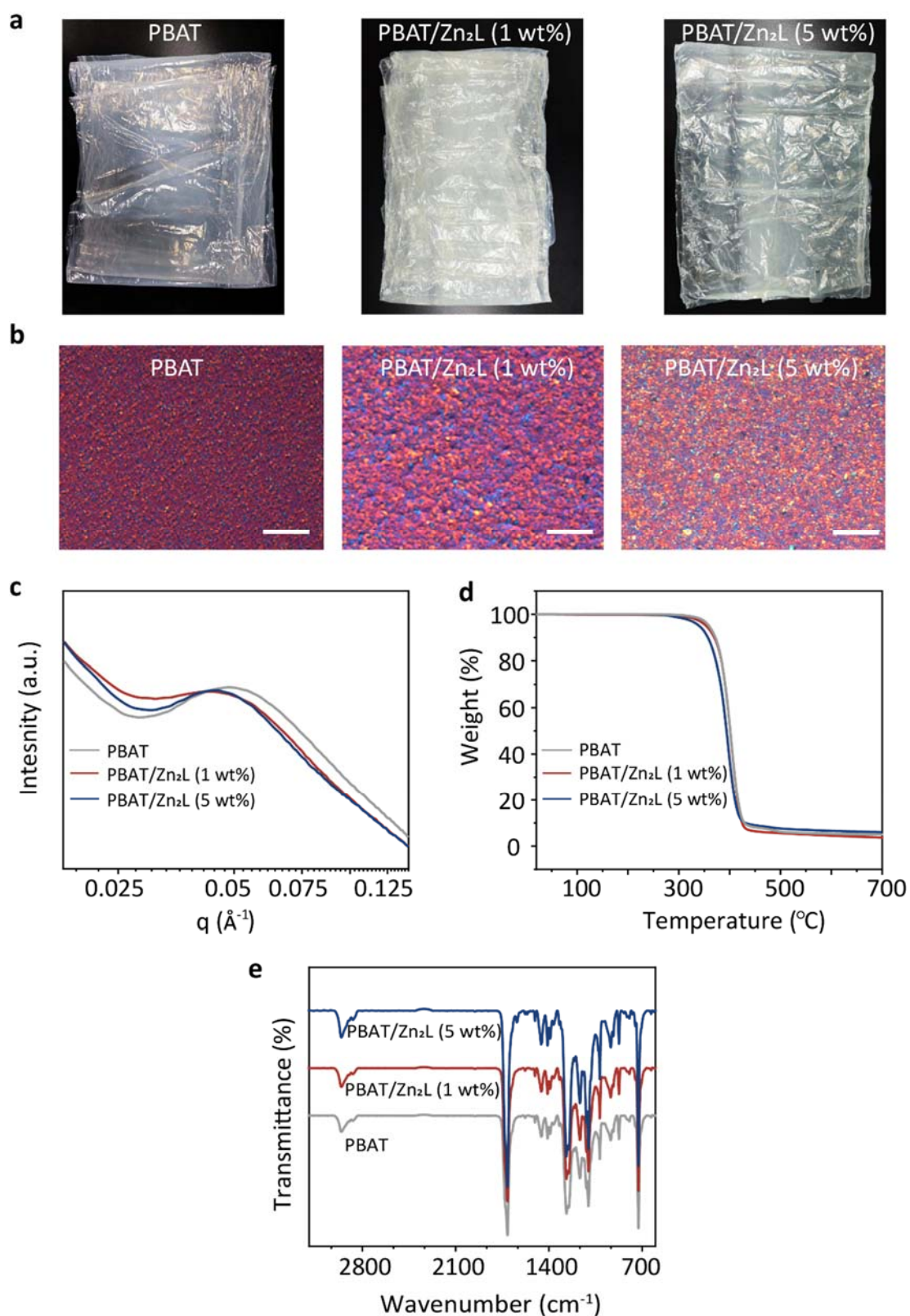


Fig. S5 Photographs (a), polarized optical microscopy images (b), small-angle X-ray scattering profiles (c), thermogravimetric analysis curves (d) and Fourier transform infrared spectra (e) of PBAT and PBAT/Zn₂L (1 and 5 wt%). Scale bar in (b): 200 μm .

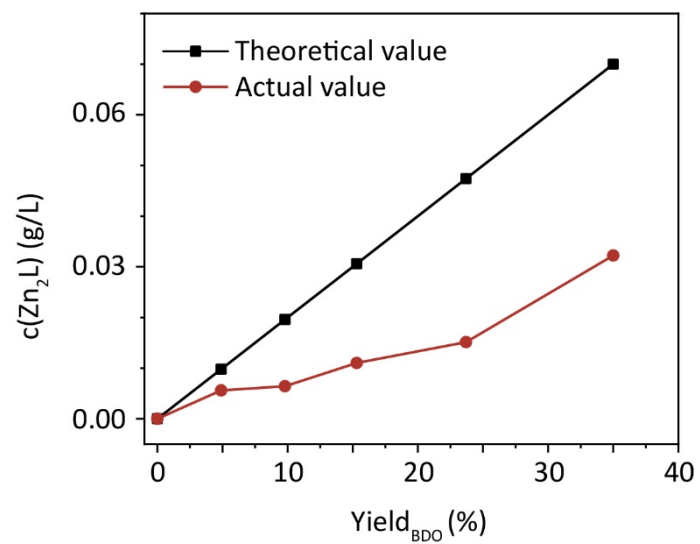


Fig. S6 The comparison of the Zn₂L concentration in solution and the theoretical value.

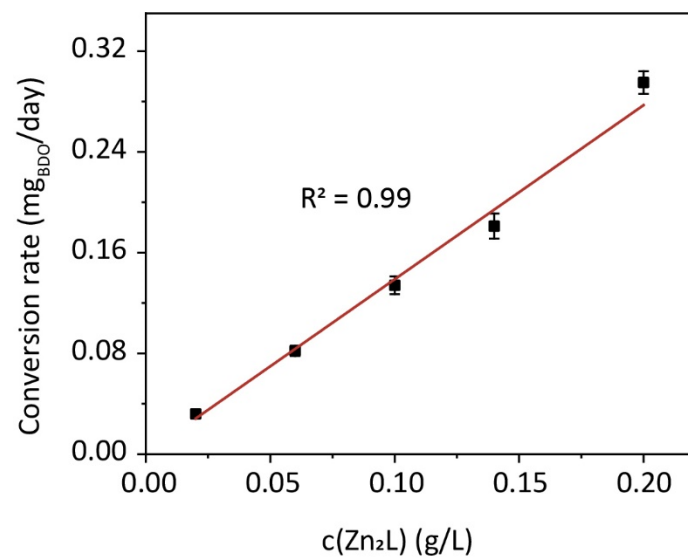


Fig. S7 The linear relationship between the Zn₂L concentration in solution and the conversion rate of PBAT.

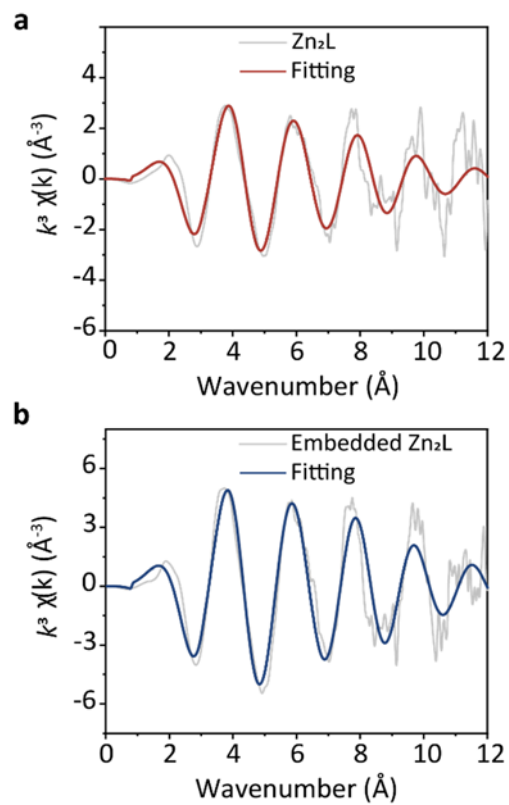


Fig. S8 The extended X-ray absorption fine structure (EXAFS) spectra in k space of the Zn K -edge of (a) free Zn_2L and (b) embedded Zn_2L .

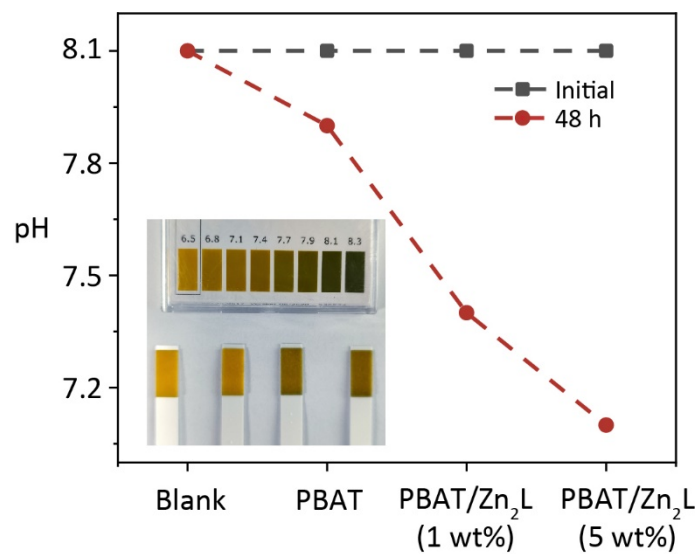


Fig. S9 The pH variations of the aqueous solutions containing PBAT film, PBAT/Zn₂L films, and the blank.

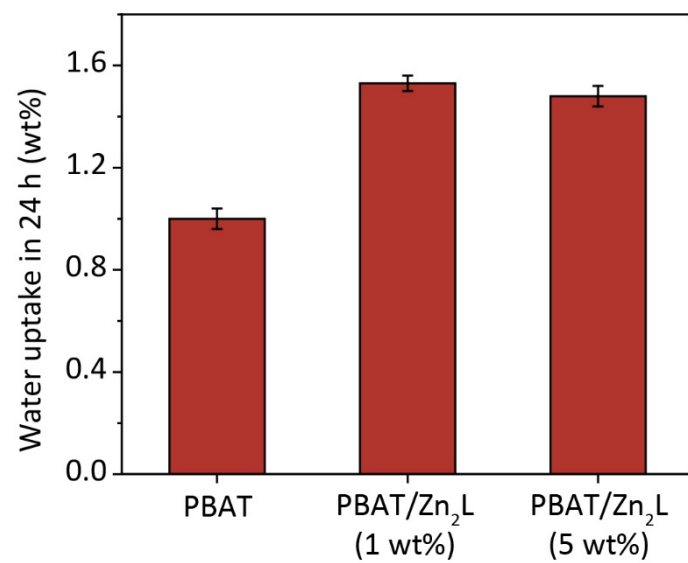


Fig. S10 Water uptake of PBAT and PBAT/Zn₂L films (1 and 5 wt%).

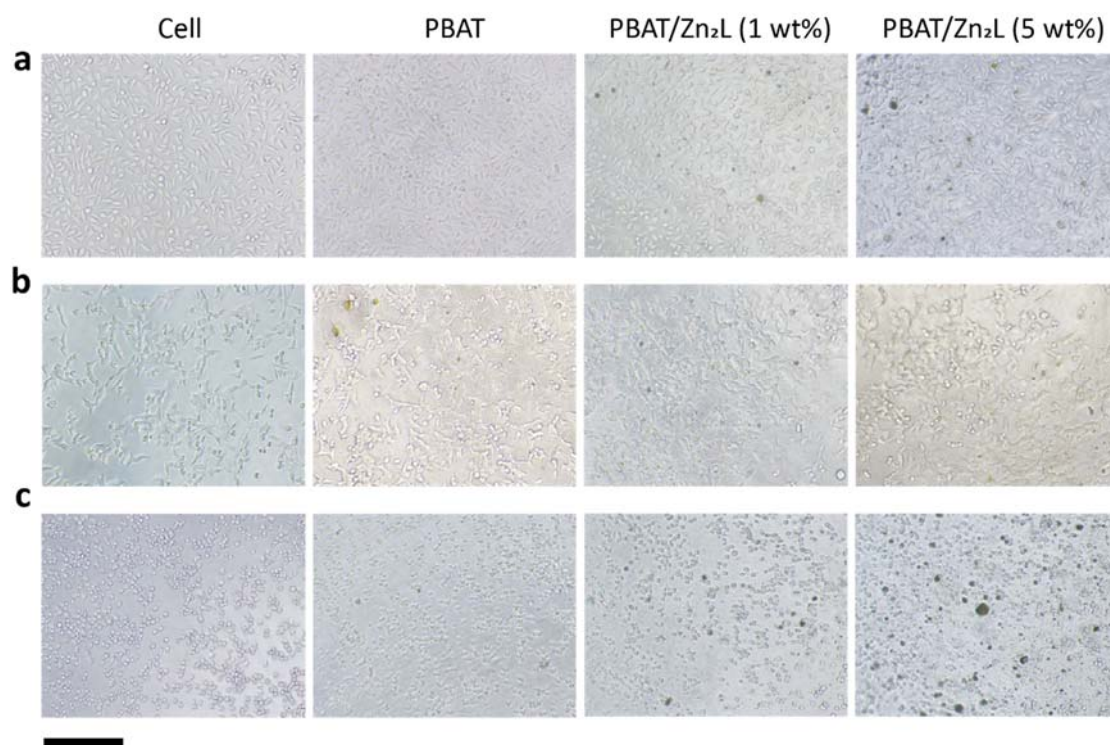


Fig. S11 Microscopic images of L929 cells (a), A549 cells (b), and RAW267.4 cells (c) without PBAT, with PBAT and PBAT/Zn₂L films, respectively. Scale bar: 200 μ m.

4. Supplementary Tables

Table S1. Data of mechanical properties of PBAT and PBAT/Zn₂L.

Sample	Tensile strength (MPa)	Elongation at break (%)	Yield strength (MPa)	Elastic modulus (MPa)
PBAT	49.4±3.4	522±14	6.5±0.8	91.3±11.0
PBAT/Zn ₂ L (1 wt%)	54.0±5.2	583±24	7.9±0.3	107.8±12.0
PBAT/Zn ₂ L (5 wt%)	46.2±3.7	609±25	7.7±0.3	108.8±8.0

Table S2. DSC data of PBAT and PBAT/Zn₂L films.

Sample	T _c (°C)	T _m (°C)	ΔH _c (J/g)	ΔH _m (J/g)	X _c (%)
PBAT	71.2	123.7	20.0	21.7	19.0
PBAT/Zn ₂ L (1 wt%)	79.2	125.4	19.4	23.1	20.4
PBAT/Zn ₂ L (5 wt%)	83.1	126.1	17.9	20.9	19.3

Table S3. SAXS data of PBAT and PBAT/Zn₂L.

Sample	q_{peak} (nm ⁻¹)	L (nm)
PBAT	0.484	13.0
PBAT/Zn ₂ L (1 wt%)	0.441	14.2
PBAT/Zn ₂ L (5 wt%)	0.427	14.7

Table S4. XAFS fitting data.

Sample	Path	CN	R (Å)	σ^2 (Å ²)	ΔE_0 (eV)	R factor
Zn(NO ₃) ₂ ·6H ₂ O	Zn-O	6.0	2.08±0.01	0.010	0.30	0.007
Zn ₂ L	Zn-O	4.9±0.3	2.03±0.01	0.012	2.54	0.010
Embedded Zn ₂ L	Zn-O	6.1±0.4	2.04±0.01	0.0073	2.50	0.009

Table S5. Characterization of composting soils.

General parameters	Soil I	Soil II
Organic carbon (g/kg)	95.9	61.2
Nitrogen (g/kg)	7.2	10.9
pH	8.2	7.4
Water holding capacity (g/kg)	628.2	655.2
Cation exchange capacity(cmol/kg)	22.7	18.9
Particle size distribution		
0.05-2.0 mm	83.6	73.4
0.002-0.05 mm	11.5	22.1
<0.002 mm	4.9	4.5

5. References

- 1 S. Zhang, Y. Xue, Y. Wu, Y.-X. Zhang, T. Tan, and Z. Niu, *Chem. Sci.*, 2023, **14**, 6558-6563.
- 2 B. Ravel, and M. Newville, *J. Synchrotron. Radiat.*, 2005, **12**, 537-541.
- 3 S. Zhang, Q. Hu, Y.-X. Zhang, H. Guo, Y. Wu, M. Sun, X. Zhu, J. Zhang, S. Gong, P. Liu and Z. Niu, *Nat. Sustain.*, 2023, **6**, 965–973.
- 4 T. Uekert, H. Kasap and E. Reisner, *J. Am. Chem. Soc.*, 2019, **141**, 15201.
- 5 T. Uekert, M. F. Kuehnel, D. W. Wakerley, and E. Reisner, *Energy Environ. Sci.*, 2018, **11**, 2853-2857.
- 6 T. Wang, Y. Shi, Y. Li, and L.-Z. Liu, *J. Polym. Eng.*, 2021, **41**, 835-841.
- 7 S. Ravati, C. Beaulieu, A. M. Zolali, and B. D. Favis, *AIChE J.*, 2014, **60**, 3005-3012.